Preterm birth accelerates the maturation of spontaneous and resting activity in the visual cortex

Isabelle F. Witteveen[1, &], Emily McCoy[1,2, &], Troy D. Holsworth[1], Catherine Z. Shen[1], Winnie Chang[3], Madelyn G. Nance[3], Allison R. Belkowitz[3], Avery Douglad[3], Meghan H. Puglia[2,3†*], Adema Ribic[1,2†*]

[1]Department of Psychology, College and Graduate School of Arts and Sciences, University of Virginia, Charlottesville, VA 22904

[2]Program in Fundamental Neuroscience, University of Virginia, Charlottesville, VA 22903

[3]Department of Neurology, School of Medicine, University of Virginia, Charlottesville, VA 22903

[&]These authors share first authorship

[†]These authors share senior authorship

***Correspondence:**
adema.ribic@virginia.edu
meghan.puglia@virginia.edu

Keywords: Preterm, Brain, Visual, Inhibition, EEG, Neuron, Activity, Aperiodic

Abstract

Prematurity is among the leading risk factors for poor neurocognitive outcomes. Brains of preterm infants often show alterations in structure, connectivity, and electrical activity, but the underlying circuit mechanisms are unclear. Using electroencephalography (EEG) in preterm and term-born infants, we find that preterm birth accelerates the maturation of aperiodic EEG components including decreased spectral power in the theta and alpha bands and flattened 1/f slope. Using *in vivo* electrophysiology in preterm mice, we find that preterm birth mice also show a flattened 1/f slope. We further found that preterm birth in mice results in suppressed spontaneous firing of neurons in the primary visual cortex, and accelerated maturation of inhibitory circuits, as assessed through quantitative immunohistochemistry. In both mice and infants, preterm birth advanced the functional maturation of the cortex. Our studies identify specific effects of preterm birth on the spectral composition of the infant EEG, and point to a potential mechanism of these effects, highlighting the utility of our parallel approach in studying the neural circuit mechanisms of preterm birth-related brain injury.

Introduction

Preterm infants born <37 weeks of gestation currently represent a tenth of the infant population, with rising prevalence. Risks for prematurity include multiple gestations and pregnancy complications, with health outcomes positively correlated with increasing age at birth (1–3). As the brain is still developing during the third postnatal month, premature birth can interrupt the developmental trajectory, resulting in multiple neurological conditions, including cerebral palsy, developmental delays, and visual deficits (4–7). Brains of preterm infants are significantly smaller and often display persistent abnormalities in functional connectivity (8–12). Neurocognitive and behavioral conditions

are common in preterm born children and adults, with a high prevalence of attention disorders and autism spectrum disorder (4,13–19). Given the increasing prevalence of preterm birth, identifying the mechanisms of preterm birth-related brain injury, along with early prognostic markers of increased risk for neurodevelopmental and neurocognitive disorders are vital for improving health outcomes of preterm individuals.

Electroencephalography (EEG) has been increasingly used in the clinical setting, both for prognostic and diagnostic purposes (20–23). EEG is non-invasive and as little as 40 s of recording is sufficient to construct basic measures of neural activity, such as neural oscillations (periodic) and background (aperiodic) neural activity (24). Both periodic and aperiodic components of the EEG power spectra show developmental changes, with spectral power decreasing in low frequency power bands and the slope of aperiodic component flattening (25–27). Both components have been used as a diagnostic and prognostic tool in the preterm population, with varying success (17,22,24,28–31). It is currently unknown how preterm birth affects EEG components in healthy preterm born infants outside of the neonatal intensive care unit (NICU) setting.

Increasing use of animal models that replicate electrophysiological signatures of preterm birth-related brain injury, such as hypoxia, has aided in identifying the cellular and circuit changes after preterm birth (32–35). Very early preterm infants and hypoxic mice share common neural deficits, such as impaired development and integration of cortical interneurons (36–39). Animal models of preterm birth itself are less commonly studied, likely due to low viability (40–42). Previous research has shown that preterm cesarean delivery does not result in neurobehavioral impairments (43), but the commonalities in electrical activity of the brain between preterm mice and preterm infants have not yet been identified.

In this study, we used EEG in healthy preterm infants and *in vivo* electrophysiology in preterm born mice to identify changes in periodic and aperiodic neural activity associated with prematurity. We focused our study on the visual brain areas, as they are well characterized anatomically and functionally in both humans and mice (44–53). We find that the aperiodic 1/f component slope is significantly flatter in both preterm infants and mice, indicating accelerated brain maturation. Using preterm mice, we identify increased inhibition in the preterm brain and point to a new mechanism that mediates preterm birth-related changes in neural activity.

Method

Infants. Sixty-eight preterm infants recruited from the University of Virginia NICU and 75 term-born infants recruited from the greater Charlottesville area completed a resting-state EEG paradigm as part of a larger, ongoing study. Infants in the NICU participated in the study as soon as their health condition was deemed sufficiently stable by their neonatology care team. Term-born infants were invited to participate from birth to 4 months of age. The primary caregiver of the infant provided written informed consent for a protocol approved by the University of Virginia (UVA) Institutional Review Board (HSR210330 or HSR19514, principal investigator: Puglia). Families were compensated $50 for their participation.

EEG acquisition and preprocessing. Resting-state EEG was recorded from 32 Ag/AgCl active actiCAP slim electrodes (Brain Products GmbH, Germany) affixed to an elastic cap according to the 10–20 electrode placement system (Figure 1A) while the infant rested in a caregiver's arms for up to 7 min. EEG was amplified with a BrainAmp DC Amplifier and recorded using BrainVision Recorder software with a sampling rate of 5000 Hz, online referenced to FCz, and online band-pass filtered

between 0.01 and 1000 Hz. Data were preprocessed with an automated preprocessing pipeline for pediatric EEG data using EEGLab v2021.1 software with quality assurance via manual inspection: data were down-sampled to 500 Hz, band-pass filtered from 0.1-100 Hz, and segmented into 10s epochs (54,55). Epochs with a voltage exceeding ± 500 µV were rejected. The data was then decomposed via independent components analysis and artifactual components (M = 6.39, SD = 3.90) were removed (56,57). Epochs with amplitude standard deviations exceeding 80 µV within a 200-ms sliding window with a 100-ms window step were discarded and problematic channels were interpolated (M = 0.84, SD = 0.83) (58). Finally, the 6 epochs with a total global field power (GFP) closest to the median GFP for each participant were selected for spectral analysis. Thirty-eight preterm and 30 term-born infants had sufficient, artifact-free data after preprocessing. An additional 11 infants (9 preterm) were excluded due to high line noise (60 Hz) contamination and mean signal amplitude < 1 µV. See Table 1 for participant demographic and perinatal characteristics.

Mice. Mice were maintained on C57BL/6 background (The Jackson Laboratory, Bar Harbor, ME) on standard 12:12 light:dark cycle, with food and water *ad libitum*. Animals from both sexes were used during the 4th week after birth. Preterm mice were generated through timed breedings, where the day after the pairing was considered as gestational day (GD) 0. Once the pregnancy was confirmed (>1.5g increase in weight at GD 10), pregnant dams were habituated to handlers by daily handling. Mifepristone (MFP, Milipore Sigma, Burlington, MA) was dissolved in DMSO and 150 µg was injected subcutaneously on GD 17. Preterm mice were delivered on GD 18. The cage with preterm mice was supplemented with external heat and occasional oxygen to prevent hypothermia and hypoxia, commonly observed in preterm mice. Control term mice were obtained from timed pregnant dams injected with DMSO only on GD 17. Animals were treated in accordance with the University of Virginia Institutional Animal Care and Use Committee guidelines.

Immunohistochemistry and imaging. Term and preterm mice (aged 35-40 days, N=3-6/group, as indicated in text and figure legends) were anesthetized with a mixture of ketamine and xylazine and transcranially perfused with warm 0.1 M phosphate buffer, followed by warm 4% paraformaldehyde (Electron Microscopy Sciences, Hatfield, PA). Brains were postfixed 1 hr at room temperature, followed by overnight fixation at 4°C. Brains were sectioned into 40 µm sections using a vibratome and stored in 1x phosphate buffered saline (PBS) and 0.01% sodium azide. For immunohistochemistry, sections were rinsed in PBS, non-specific binding was blocked with 3% normal horse serum (heat inactivated, ThermoFisher, Waltham, MA) and 0.3% Triton-X 100 (Sigma-Aldrich) in PBS (sterile filtered). Antibodies were incubated overnight at 4°C. Parvalbumin (anti-goat) was used at 1/200 (Swant, Belinzona, Switzerland) and detected with donkey anti-goat Alexa 647 (ThermoFisher). NeuN and GAD65/67 were both anti-rabbit (Milipore Sigma) and were used with secondary NanoTag reagents (FluoTag X2 Atto 488 and Alexa 647) according to the manufacturer's protocol (NanoTag Biotechnologies, GmbH, Goettingen, Germany). After staining, sections were rinsed in distilled water, mounted on glass slides, briefly dried, and coverslipped with Aquamount (Polysciences, Warrington, PA). Images were acquired using Zeiss LSM 800 at 2048x2048 resolution. Single optical sections from the visual cortex using 63x 1.2 NA C-Apochromat were acquired for GAD65/67 quantification, and z-stacks were acquired using 40x1.2 NA Plan-Apochromat for Parvalbumin intensity quantification. Images were collected from 4-6 sections/mouse (minimum 20 images/mouse). Quantification was performed on background subtracted images using ImageJ. Automatic thresholding was applied to GAD65/67 images before using the puncta analyzer function on NeuN-outlined neuronal cell bodies.

In vivo electrophysiology in mice. Recordings were performed on awake term and preterm (N=9 and 6, respectively) female and male mice, ages 21 to 28 days after birth, using a treadmill as described in

(Niell and Stryker, 2010). Four to seven days before the recording session, custom made stainless steel head-plate implants were cemented to the mouse skull. Animals were anesthetized with isoflurane in oxygen (2% induction, 1.0–1.8% maintenance), warmed with a heating pad at 38°C and given subcutaneous injections of Buprenorphine SR (1mg/kg) and 0.25% Bupivacaine (locally). Eyes were covered with Puralube (Decra, Northwich, UK). Scalp and fascia from Bregma to behind lambda were removed, and the skull was cleaned, dried and covered with a thin layer of Scotchbond adhesive (3M, Maplewood, MN). Skin edges were sealed with VetBond (3M). The head plate was attached with dental cement (RelyX Ultimate, 3M). The well of the head plate was filled with silicone elastomer (Reynold Advanced Materials, Brighton, MA) to protect the skull before recordings. Animals were group housed after the implantation and monitored daily for signs of shock or infection. Two to three days before the recording, the animals underwent one to two 20-30 minutes handling sessions and one to two 10-20 minutes sessions in which the animals were habituated to the treadmill (Dombeck et al., 2007). On the day of recording, the animals were anesthetized as above and small craniotomies (~0.5 mm in diameter) with 18G needles were made above V1 (2-3 mm lateral to midline, 0.5-1 mm anterior to lambda) and cerebellum. The brain surface was covered in 2-3% low melting point agarose (Promega, Madison, WI) in sterile saline and then capped with silicone elastomer. Animals were allowed to recover for 2–4 h. For the recording sessions, mice were placed in the head-plate holder above the treadmill and allowed to habituate for 5-10 minutes. The agarose and silicone plug were removed, the reference insulated silver wire electrode (A-M Systems, Carlsborg, WA) was placed in cerebellum and the well was covered with warm sterile saline. A multisite electrode spanning all cortical layers (A1x16-5mm-50-177-A16; Neuronexus Technologies, Ann Arbor, MI) was coated with DiI (Invitrogen) to allow post hoc insertion site verification and then inserted in the brain through the craniotomy. The electrode was lowered until the uppermost recording site had entered the brain and allowed to settle for 20-30 minutes. The well with the electrode was then filled with 3% agarose to stabilize the electrode and the whole region was kept moist with surgical gelfoam soaked in sterile saline (Pfizer, MA). Minimum 2 penetrations were made per animal to ensure proper sampling of the craniotomy. After the recording, mice were euthanized with an overdose of ketamine and xylazine or kept for subsequent experiments after protecting the craniotomy with silicone elastomer.

Data collection and analysis for mice. Blank screen was generated with MATLAB (MathWorks, Natick, MA) using the Psychtoolbox extension (Brainard, 1997) and presented on a gamma corrected 27” LCD. The screen was centered 25 cm from the mouse's eye, covering ~80° of visual space. The signals were sampled at 25 kHz using Spike2 and data acquisition unit (Power 1401-3, CED). Signals were fed into a 16-channel amplifier (Model 3500; A-M Systems), amplified 200x and band-pass filtered 0.7-7000 Hz. Only stationary, non-running stages were analyzed offline using Spike2 software (CED). For single unit analysis, spikes were extracted from band-pass filtered data (all 16 channels) using thresholds (3x standard deviation) and sorted in Spike 2. For spectral analyses, layer 2/3 was selected due to its high correlation with EEG signal (59). 60 s epochs of data during viewing of the blank screen were selected and downsampled to 500 Hz prior to spectral analysis to match the infant data.

Quantification and statistical analysis. All analyses were performed with the researchers blind to the condition. Statistical analyses were performed in GraphPad Prism 9.0 (GraphPad Inc., La Jolla, USA) using nested t-test and one or two-way ANOVA with post-hoc comparisons (as indicated in text and figure legends), unless stated otherwise. Spectral analysis was performed with Spike2 on 60 s of data at 500 Hz for both infant and mouse datasets. Power was normalized to the power in high frequency band (150-250 Hz). Power spectral density values were averaged across channels of interest (Figure 1A). 1/f slope was generated using linear regression from 0.1-100 Hz after log-transform of

frequency and power. All data are reported as mean ± SEM, where N represents number of animals and infants used, unless indicated otherwise. Target power for all sample sizes was 0.8. In all cases, alpha was set to 0.05.

Results

Neurocognitive and visual deficits are common in preterm children (60–65), but they are often diagnosed in school age, precluding early interventions (66–68). To identify early postnatal biomarkers of impaired activity in visual areas, we used electroencephalography (EEG) to measure resting state activity in the occipital and parietal visual areas within the first 4 months of life in preterm and term-born infants. All data were collected prior to the onset of the critical period for the development of binocularity at 6 months of age (69), a visual function that is highly sensitive to altered perinatal experience (69–71). Sixty seconds of resting state EEG data from occipital and parietal electrodes (Figure 1A) were collected from 29 preterm and 28 term infants. While the preterm infants had a typical distribution of high power in low frequencies and low power in high frequencies (Figure 1 B-C), power in theta and alpha bands was significantly reduced in preterm infants (Figure 1B).

As visual function matures earlier in preterm infants (71), we then asked if the electrophysiological activity of the visual cortex would reflect this accelerated maturation. To test this, we calculated the slope of aperiodic EEG component 1/f (Figure 1C). 1/f is thought to reflect the background activity of the brain (72), and 1/f slopes become progressively flatter during infancy (25). As previously reported (25), we found that the power spectra of term and preterm infants were largely aperiodic (Figure 1C). However, we found that preterm infants had a significantly flatter 1/f slope when compared to term infants, despite preterm infants being significantly younger in postmenstrual age ($t(55) = -6.66$, $p < .001$) and equivalent in chronological age ($t(55) = -0.75$, $p = .455$, see also Table 1). These results confirmed accelerated maturation of visual areas in preterm infants (71).

To study the effects of preterm birth on the maturation of visual areas in cellular details, we used prematurely-born mice as a model of preterm birth (73). Preterm mice were generated through subcutaneous injections of progesterone antagonist mifepristone (MFP) to timed-pregnant dams at GD 17 (Figure 2A)(41). Preterm mice are born a 0.75-1 day early (depending on the precise parturition time), have a significantly lower birth weight (Figure 2B), and increased mortality rates due to hypothermia, hypoxia, and inability to suckle (1-3 pups/litter). However, surviving pups are otherwise viable and display a catch-up growth typical of preterm-born infants (Figure 2C) (74). Preterm mice open their eyes significantly earlier, further suggesting accelerated development of visual brain areas after preterm birth (Figure 2D). To confirm that electrophysiological activity of visual areas in preterm mice recapitulates changes seen in preterm infants (Figure 1C) , we used *in vivo* electrophysiology to record intracortical local field potentials (LFPs) in layer 2/3 of the primary visual cortex (V1) of awake, young term and preterm mice (Figure 2E) (75). We used mice in their fourth week of postnatal development as that period represents the onset of the critical period for binocular maturation in mice (76). There was a significant interaction between the timing of birth and the energy composition of the power spectra (Figure 2F), but post-hoc tests revealed no significant differences within any of the power bands, likely due to lower number of mice used for the experiments (Figure 2F, compare to Figure 1B). However, preterm mice also had a significantly flatter 1/f slope (Figure 2G), indicating accelerated maturation of the primary visual cortex and suggesting the relative conservation of the effects of prematurity on neural activity in mice and humans.

The fourth postnatal week represents a critical transition towards visually-driven activity in mice, reflected in increasing suppression of spontaneous activity by rising levels of inhibitory neurotransmission (51,77). Given the flatter, "older" 1/f slope in preterm mice (Figure 2F-G), we hypothesized that the spontaneous firing rates of visual cortex neurons would be lower in preterm mice reflecting accelerated transition to visually-driven activity. We isolated single unit responses from all layers of the cortex (Figure 3A) and estimated their firing rates in stationary, awake mice whose eyes were centered on a blank, grey screen (Figure 2E). We indeed found a significantly reduced spontaneous firing rate of visual cortex neurons in preterm mice (Figure 3B). To probe the cellular mechanism of reduced spontaneous firing in preterm mice, we quantified the expression of inhibitory synapse marker glutamic acid decarboxylase 65/67 (GAD65/67) (78–80). The number and size of perisomatic GAD65/67 puncta are a reliable indicator of inhibitory neurotransmission levels (80). In agreement with suppressed spontaneous activity in preterm visual cortex, the size of perisomatic GAD65/67 puncta was significantly increased in preterm mice (Figure 3 E-D), with no changes in their density (Term=15.62±0.4, Preterm=14.98±0.88 puncta/100 μm^2 of NeuN+ soma; N=6 and 5 mice). Cortical perisomatic inhibition is mediated by fast-spiking, Parvalbumin-expressing interneurons (81). As previous studies of preterm birth-related brain injury models reported changes in Parvalbumin interneuron distribution and density (36,37,82), we then asked if this neuronal population is affected by preterm birth. Cortical interneurons represent a mixture of high, middle and low Parvalbumin (PV)-expressing interneurons (83), with low PV interneurons being the dominant group in the developing brain and high PV in the mature brain (83). In agreement with accelerated maturation of the visual cortex, preterm mice had a significantly higher proportion of high PV interneurons (Figure 3 E-F), without any changes in the overall density of PV interneurons (Term=22.45±3.53, Preterm=23.79±2.56 PV interneurons per field of view, N=5 term and 3 preterm mice). Altogether, these results demonstrate accelerated maturation of the visual cortex after preterm birth and suggest a central role of inhibition in this process.

Discussion

Despite extensive research, effects of premature birth on cortical activity in the early postnatal period remain unclear. Through a comparative approach, our study identifies accelerated maturation of neural activity in the visual cortex of preterm infants and mice. Our study further suggests that elevated levels of inhibition are central to mediating the changes in neural activity after preterm birth.

Cortical oscillatory activity shows distinct developmental patterns, with a reduction in the relative power of low frequencies and an increase in high frequencies with increasing age (26,84). Such distribution of powers is likely responsible for the age-related flattening of 1/f EEG slope (25,27). An "older" spectral profile in preterm infants and mice is in agreement with the notion that premature exposure to extrauterine environment accelerates brain maturation, at least in primary sensory areas such as the visual cortex (71). As primary sensory areas mature earlier than the frontal executive and association areas (85), it will be important to determine if the accelerated maturation of sensory areas impairs the sequence of cortical maturation, especially considering the high prevalence of executive function disorders in preterm children (86,87).

Fast-spiking, Parvalbumin interneurons are central for the maturation of cortical circuits (85,88). Their functional development is sensitive to experience and in the visual cortex, their maturation can be accelerated or delayed through manipulations of visual input (89–91). In agreement, our results suggest that premature onset of visual input can accelerate the maturation of cortical Parvalbumin interneurons, shifting their distribution to high-PV expressing interneurons in preterm mice. Previous studies of hypoxic mouse models of preterm birth have demonstrated that hypoxia results in reduced density of Parvalbumin interneurons, as well as in an increase in the intensity of Parvalbumin signal

(91). The differing findings in our study are likely due to low or absent hypoxia in our mouse model, as well as differences in how the preterm brain injury is modelled. Hypoxia models of preterm birth are commonly term-born, with continuous or intermittent exposure to hypoxia during the postnatal development (38,91–93). While hypoxia represents a severe injury, it may not recapitulate the effects of preterm birth alone. Birth itself is an environmental shock that can significantly affect neuronal and synaptic development (73,94). As the effects of preterm birth in the absence of other pathologies are unclear, our results highlight a need for multiple animal models to capture the variability in the degree of preterm birth-related brain injury.

Another potential cause of divergence between our findings in preterm mice and previously published findings on interneuronal populations (38,95) in preterm infant cortex is the degree of prematurity. The most vulnerable population of preterm infants are born extremely early, prior to week 28 of gestation, and very early (28-32 weeks of gestation). These are also the infants that show deficits in cortical interneurons (36,38,95,96). Yet, the majority (>70%) of preterm infants are born moderately to late preterm (32-37 weeks of gestation), with variable degrees of health complications, including hypoxic brain injury (97,98). Infants in our study reflect this, with 51.7% born moderately to late preterm (Table 1). Considering the relatively high viability of preterm mice, our results suggest that mice born a day early are a model of middle to late preterm birth. As early and late preterm infants have similarly poor neurocognitive outcomes (18,67,86,97), our study points to potentially divergent neural circuit mechanisms of impaired brain function in early and late preterm infants.

Term-born mouse pups in the first postnatal week are commonly compared to preterm newborns, based on cortical development milestones (52,99). While direct comparison between developmental stages of mice and humans is difficult due to different rates of maturation, our results confirm previous findings of accelerated brain maturation after premature birth (73,94). Our results further highlight the utility of simple EEG measures in the clinical setting and set the stage for future longitudinal studies that will explore the relationship between 1/f slope and neurodevelopmental outcomes in the preterm population. Our study adds to the growing body of evidence that birth itself is a critical transition in brain development. Future studies will undoubtedly explore how the timing of this transition affects sensory and cognitive processing, given that preterm infants are at higher risk for developing neurodevelopmental and neuropsychiatric disorders (87).

Conflict of Interest

The authors declare that the research was conducted in the absence of any commercial or financial relationships that could be construed as a potential conflict of interest.

Author Contributions

AR and MHP conceived and designed the study. AR acquired and analyzed data collected from mice, and MHP, MN, WC, AB, and AD acquired and analyzed data collected from infants. EM analyzed data collected from mice and infants. IW, TDH and CS collected and analyzed the immunohistochemistry data. AR wrote the manuscript with input from all authors.

Funding

AR, IW, TDH, CS and EM are funded through the Department of Psychology at the University of Virginia. Research reported in this publication was supported in part by the National Center For Advancing Translational Sciences of the National Institutes of Health under Award Numbers

KL2TR003016/ULTR003015 to AR, The National Institutes of Mental Health K01MH125173 to MHP, and The Jefferson Trust Foundation to MHP. The content is solely the responsibility of the authors and does not necessarily represent the official views of the National Institutes of Health.

Acknowledgments

The authors would like to thank the Cang and Liu labs at the Departments of Biology and Psychology for generous access to their confocal microscope, Drs. Zanelli and Fairchild at the University of Virginia Children's Hospital for their assistance identifying candidate participants in the NICU, and the participating families for taking part in our research.

Data Availability Statement

The datasets generated and analyzed in this study will be provided upon reasonable request.

Table 1. Participant demographic and perinatal characteristics

	Preterm infants (n = 29)	**Term infants** (n = 28)
GA (weeks), mean ± SD	31.4 ± 3.4	39.2 ± 0.9
Extremely preterm (<28 weeks)	6 (20.7%)	-
Very preterm (28-32 weeks)	8 (27.6%)	-
Moderate preterm (32-34 weeks)	4 (13.8%)	-
Late preterm (34-37 weeks)	11 (37.9%)	-
Early term (37-39 weeks)	-	6 (21.4%)
Full term (39-41 weeks)	-	22 (78.6%)
Late term (>41 weeks)	-	-
PMA at test (weeks), mean ± SD	39.0 ± 5.4	47.9 ± 4.6
CA at test (weeks), mean ± SD	7.5 ± 6.8	8.7 ± 4.4
Sex		
Female (%)	16 (55%)	15 (54%)
Male (%)	13 (45%)	13 (46%)
Race		
White (%)	23 (79%)	21 (75%)
Black (%)	5 (17%)	1 (3.5%)
More than 1 race (%)	1 (3%)	5 (18%)
Unknown race (%)	-	1 (3.5%)
Delivery method		
Vaginal (%)	9 (31%)	18 (71%)

Cesarean (%)	20 (69%)	7 (25%)
Unknown	-	1 (4%)
Birth weight (grams), mean□±□SD	1681 (664)	3652 (817)*
SGA (%)	6 (20%)	-*
APGAR at 5 min, median (min, max)	7 (2, 8)	8 (6, 9)*

Data are expressed as sample size unless otherwise stated. GA, gestational age; PMA, postmenstrual age; CA, chronological age; SGA, small for gestational age, defined as < 10th percentile.
*Birthweight was not available for 1 term infant; Apgar scores were not available for 4 term infants.

Figure legends

Figure 1. A) EEG cap montage. Highlighted parietal and occipital channels are analyzed. **B)** Preterm birth significantly reduces resting theta and alpha band power. Two-way ANOVA interaction: p=0.039; F (4, 220) = 2.55; N= 29 preterm and 28 term-born infants. Sidak's multiple comparisons test: theta p<.0001, alpha p=.022. **C)** Preterm infants have a significantly flatter slope of log transformed 2-25 Hz power. Linear regression; slope and r^2 values are indicated. Data shown as mean or mean±SEM.

Figure 2. Preterm mice display a flatter slope of aperiodic LFP component. A) Preterm mice are generated through the injection of Mifepristone (dissolved in DMSO) to pregnant dams at postconceptional day 17. Dams deliver pups within 24 hrs (1 day early: postnatal day/P 0). Term controls are generated by injecting pregnant dams at postconceptional day 17 with DMSO. **B)** Preterm pups show a significantly lower birth weight (N=29 term and 37 preterm mice, t-test, $t(64)=5.63$, $p<0.0001$) and **C)** an accelerated postnatal growth rate (ordinary two-way ANOVA, $F(1, 433) = 98.53$, $p<0.0001$; N=29 term and 19 preterm mice and **D)** precocious eye opening (t-test, $t(25)=7.95$, $p<0.0001$; N=16 term and 11 preterm mice). **E)** Schematics of in vivo electrophysiology in awake mice. Local field potentials (LFPs) are collected using linear silicone probes (Neuronexus). Scale bar: 10 µV and 0.1 s. **F)** Preterm birth significantly affects the distribution of power across different frequency bands (two-way ANOVA, F(4, 56) = 2.568, p = .048; N=6 preterm and 10 term and mice). G) Preterm mice show a significantly flatter slope of log transformed 2-70 Hz power. Linear regression; slope and r^2 values are indicated. Data shown as mean or mean±SEM.

Figure 3. Preterm mice show elevated inhibition in the visual cortex. A) Top: raw LFP trace; middle: filtered 0.7-7 kHz LFP; bottom: identified single units. **B)** Preterm mice have a significantly reduced firing rate of neurons in the visual cortex during the presentation of a blank grey screen. 239 units from N=5 term and 6 preterm mice, nested t-test, $t(9)=2.428$, $p=.038$. Data shown as mean or mean±SEM. **C)** Immunohistochemical detection of NeuN (yellow) and GAD65/67 (cyan) in the visual cortex of term and preterm mice. Arrowheads: putative inhibitory synapses. **D)** Cumulative frequency distribution of puncta size in term and preterm mice shows a significant shift to the right in term mice, signifying increased puncta size across all synaptic populations. Kolmogorov-Smirnov test, p<.001. Minimum 100 NeuN cell bodies/mouse from N=5 preterm and 6 term mice. **E)** Representative maximum projections of brain sections stained for Parvalbumin and quantified for Parvalbumin intensity. **F)** Cumulative distribution of Parvalbumin intensity measurements from. The curve in preterm mice is shifter to the right, demonstrating the significantly increased intensity of Parvalbumin staining in preterm mice. N=477 and 636 cell bodies from 3 preterm and 6 term mice, respectively. Kolmogorov-Smirnov test, p<.001.

Bibliography

1. Blencowe H, Cousens S, Oestergaard MZ, Chou D, Moller A-B, Narwal R, et al. National, regional, and worldwide estimates of preterm birth rates in the year 2010 with time trends since 1990 for selected countries: a systematic analysis and implications. Lancet. 2012 Jun 9;379(9832):2162–2172.

2. Blencowe H, Lee ACC, Cousens S, Bahalim A, Narwal R, Zhong N, et al. Preterm birth-associated neurodevelopmental impairment estimates at regional and global levels for 2010. Pediatr Res. 2013 Dec;74 Suppl 1:17–34.

3. Barfield WD. Public health implications of very preterm birth. Clin Perinatol. 2018 Sep;45(3):565–577.

4. Limperopoulos C, Bassan H, Gauvreau K, Robertson RL, Sullivan NR, Benson CB, et al. Does cerebellar injury in premature infants contribute to the high prevalence of long-term cognitive, learning, and behavioral disability in survivors? Pediatrics. 2007 Sep;120(3):584–593.

5. Ortinau C, Neil J. The neuroanatomy of prematurity: normal brain development and the impact of preterm birth. Clin Anat. 2015 Mar;28(2):168–183.

6. Leung MP, Thompson B, Black J, Dai S, Alsweiler JM. The effects of preterm birth on visual development. Clin Exp Optom. 2018 Jan;101(1):4–12.

7. Mann JR, McDermott S, Griffith MI, Hardin J, Gregg A. Uncovering the complex relationship between pre-eclampsia, preterm birth and cerebral palsy. Paediatr Perinat Epidemiol. 2011 Mar;25(2):100–110.

8. Bouyssi-Kobar M, Brossard-Racine M, Jacobs M, Murnick J, Chang T, Limperopoulos C. Regional microstructural organization of the cerebral cortex is affected by preterm birth. Neuroimage Clin. 2018 Mar 16;18:871–880.

9. Bouyssi-Kobar M, du Plessis AJ, McCarter R, Brossard-Racine M, Murnick J, Tinkleman L, et al. Third trimester brain growth in preterm infants compared with in utero healthy fetuses. Pediatrics. 2016 Nov;138(5).

10. Pandit AS, Robinson E, Aljabar P, Ball G, Gousias IS, Wang Z, et al. Whole-brain mapping of structural connectivity in infants reveals altered connection strength associated with growth and preterm birth. Cereb Cortex. 2014 Sep;24(9):2324–2333.

11. Hunt BAE, Scratch SE, Mossad SI, Emami Z, Taylor MJ, Dunkley BT. Disrupted visual cortex neurophysiology following very preterm birth. Biol Psychiatry Cogn Neurosci Neuroimaging. 2019 Sep 16;

12. Tokariev A, Stjerna S, Lano A, Metsäranta M, Palva JM, Vanhatalo S. Preterm birth changes networks of newborn cortical activity. Cereb Cortex. 2019 Feb 1;29(2):814–826.

13. Strang-Karlsson S, Andersson S, Paile-Hyvärinen M, Darby D, Hovi P, Räikkönen K, et al. Slower reaction times and impaired learning in young adults with birth weight <1500 g. Pediatrics. 2010 Jan;125(1):e74–82.

14. Treyvaud K, Ure A, Doyle LW, Lee KJ, Rogers CE, Kidokoro H, et al. Psychiatric outcomes at age seven for very preterm children: rates and predictors. J Child Psychol Psychiatry. 2013 Jul;54(7):772–779.

15. Del Hoyo Soriano L, Rosser T, Hamilton D, Wood T, Abbeduto L, Sherman S. Gestational age is related to symptoms of attention-deficit/hyperactivity disorder in late-preterm to full-term children and adolescents with down syndrome. Sci Rep. 2020 Nov 23;10(1):20345.

16. Jaekel J, Wolke D, Bartmann P. Poor attention rather than hyperactivity/impulsivity predicts academic achievement in very preterm and full-term adolescents. Psychol Med. 2013 Jan;43(1):183–196.

17. Shuffrey LC, Pini N, Potter M, Springer P, Lucchini M, Rayport Y, et al. Aperiodic electrophysiological activity in preterm infants is linked to subsequent autism risk. Dev Psychobiol. 2022 May;64(4):e22271.

18. Crump C, Sundquist J, Sundquist K. Preterm or early term birth and risk of autism. Pediatrics. 2021 Sep;148(3).

19. McGowan EC, Sheinkopf SJ. Autism and preterm birth: clarifying risk and exploring mechanisms. Pediatrics. 2021 Sep;148(3).

20. Holmes GL, Lombroso CT. Prognostic value of background patterns in the neonatal EEG. J Clin Neurophysiol. 1993 Jul;10(3):323–352.

21. Rivera MJ, Teruel MA, Maté A, Trujillo J. Diagnosis and prognosis of mental disorders by means of EEG and deep learning: a systematic mapping study. Artif Intell Rev. 2021 Mar 27;

22. Watanabe K, Hayakawa F, Okumura A. Neonatal EEG: a powerful tool in the assessment of brain damage in preterm infants. Brain and Development. 1999 Sep;21(6):361–372.

23. McCoy B, Hahn CD. Continuous EEG monitoring in the neonatal intensive care unit. J Clin Neurophysiol. 2013 Apr;30(2):106–114.

24. O'Toole JM, Boylan GB. Quantitative preterm EEG analysis: the need for caution in using modern data science techniques. Front Pediatr. 2019 May 3;7:174.

25. Schaworonkow N, Voytek B. Longitudinal changes in aperiodic and periodic activity in electrophysiological recordings in the first seven months of life. Dev Cogn Neurosci. 2021 Feb;47:100895.

26. Gasser T, Verleger R, Bächer P, Sroka L. Development of the EEG of school-age children and adolescents. I. Analysis of band power. Electroencephalogr Clin Neurophysiol. 1988 Feb;69(2):91–99.

27. Saby JN, Marshall PJ. The utility of EEG band power analysis in the study of infancy and early childhood. Dev Neuropsychol. 2012;37(3):253–273.

28. Lloyd RO, O'Toole JM, Livingstone V, Filan PM, Boylan GB. Can EEG accurately predict 2-year neurodevelopmental outcome for preterm infants? Arch Dis Child Fetal Neonatal Ed. 2021 Sep;106(5):535–541.

29. Vanhatalo S, Tallgren P, Andersson S, Sainio K, Voipio J, Kaila K. DC-EEG discloses prominent, very slow activity patterns during sleep in preterm infants. Clin Neurophysiol. 2002 Nov;113(11):1822–1825.

30. Nishiyori R, Xiao R, Vanderbilt D, Smith BA. Electroencephalography measures of relative power and coherence as reaching skill emerges in infants born preterm. Sci Rep. 2021 Feb 11;11(1):3609.

31. Nordvik T, Schumacher EM, Larsson PG, Pripp AH, Løhaugen GC, Stiris T. Early spectral EEG in preterm infants correlates with neurocognitive outcomes in late childhood. Pediatr Res. 2022 Oct;92(4):1132–1139.

32. Zanelli S, Goodkin HP, Kowalski S, Kapur J. Impact of transient acute hypoxia on the developing mouse EEG. Neurobiol Dis. 2014 Aug;68:37–46.

33. Burnsed J, Skwarzyńska D, Wagley PK, Isbell L, Kapur J. Neuronal Circuit Activity during Neonatal Hypoxic-Ischemic Seizures in Mice. Ann Neurol. 2019 Dec;86(6):927–938.

34. El-Hayek YH, Wu C, Zhang L. Early suppression of intracranial EEG signals predicts ischemic outcome in adult mice following hypoxia-ischemia. Exp Neurol. 2011 Oct;231(2):295–303.

35. Johnson KJ, Moy B, Rensing N, Robinson A, Ly M, Chengalvala R, et al. Functional neuropathology of neonatal hypoxia-ischemia by single-mouse longitudinal electroencephalography. Epilepsia. 2022 Dec;63(12):3037–3050.

36. Stolp HB, Fleiss B, Arai Y, Supramaniam V, Vontell R, Birtles S, et al. Interneuron development is disrupted in preterm brains with diffuse white matter injury: observations in mouse and human. Front Physiol. 2019 Jul 30;10:955.

37. Scheuer T, dem Brinke EA, Grosser S, Wolf SA, Mattei D, Sharkovska Y, et al. Reduction of cortical parvalbumin-expressing GABAergic interneurons in a rodent hyperoxia model of preterm birth brain injury with deficits in social behavior and cognition. Development. 2021 Oct 15;148(20).

38. Lacaille H, Vacher C-M, Bakalar D, O'Reilly JJ, Salzbank J, Penn AA. Impaired interneuron development in a novel model of neonatal brain injury. eNeuro. 2019 Feb 22;6(1).

39. Malik S, Vinukonda G, Vose LR, Diamond D, Bhimavarapu BBR, Hu F, et al. Neurogenesis continues in the third trimester of pregnancy and is suppressed by premature birth. J Neurosci. 2013 Jan 9;33(2):411–423.

40. Elovitz MA, Mrinalini C. Animal models of preterm birth. Trends Endocrinol Metab. 2004 Dec;15(10):479–487.

41. Dudley DJ, Branch DW, Edwin SS, Mitchell MD. Induction of preterm birth in mice by RU486. Biol Reprod. 1996 Nov;55(5):992–995.

42. McCarthy R, Martin-Fairey C, Sojka DK, Herzog ED, Jungheim ES, Stout MJ, et al. Mouse models of preterm birth: suggested assessment and reporting guidelines. Biol Reprod. 2018 Nov 1;99(5):922–937.

43. Chiesa M, Guimond D, Tyzio R, Pons-Bennaceur A, Lozovaya N, Burnashev N, et al. Term or Preterm Cesarean Section Delivery Does Not Lead to Long-term Detrimental Consequences in Mice. Cereb Cortex. 2019 Jun 1;29(6):2424–2436.

44. Kiorpes L. The puzzle of visual development: behavior and neural limits. J Neurosci. 2016 Nov 9;36(45):11384–11393.

45. Huttenlocher PR, de Courten C, Garey LJ, Van der Loos H. Synaptogenesis in human visual cortex--evidence for synapse elimination during normal development. Neurosci Lett. 1982 Dec 13;33(3):247–252.

46. Pinto JGA, Hornby KR, Jones DG, Murphy KM. Developmental changes in GABAergic mechanisms in human visual cortex across the lifespan. Front Cell Neurosci. 2010 Jun 10;4:16.

47. Haak KV, Morland AB, Engel SA. Plasticity, and its limits, in adult human primary visual cortex. Multisens Res. 2015;28(3-4):297–307.

48. Norcia AM, Tyler CW, Piecuch R, Clyman R, Grobstein J. Visual acuity development in normal and abnormal preterm human infants. J Pediatr Ophthalmol Strabismus. 1987 Apr;24(2):70–74.

49. Lunghi C, Burr DC, Morrone C. Brief periods of monocular deprivation disrupt ocular balance in human adult visual cortex. Curr Biol. 2011 Jul 26;21(14):R538–9.

50. Mitchell DE, Maurer D. Critical periods in vision revisited. Annu Rev Vis Sci. 2022 Sep 15;8:291–321.

51. Shen J, Colonnese MT. Development of activity in the mouse visual cortex. J Neurosci. 2016 Nov 30;36(48):12259–12275.

52. Colonnese MT, Kaminska A, Minlebaev M, Milh M, Bloem B, Lescure S, et al. A conserved switch in sensory processing prepares developing neocortex for vision. Neuron. 2010 Aug 12;67(3):480–498.

53. Antonini A, Fagiolini M, Stryker MP. Anatomical correlates of functional plasticity in mouse visual cortex. J Neurosci. 1999 Jun 1;19(11):4388–4406.

54. Puglia MH, Slobin JS, Williams CL. The automated preprocessing pipe-line for the estimation of scale-wise entropy from EEG data (APPLESEED): Development and validation for use in pediatric populations. Dev Cogn Neurosci. 2022 Dec;58:101163.

55. Delorme A, Makeig S. EEGLAB: an open source toolbox for analysis of single-trial EEG dynamics including independent component analysis. J Neurosci Methods. 2004 Mar 15;134(1):9–21.

56. Debnath R, Buzzell GA, Morales S, Bowers ME, Leach SC, Fox NA. The Maryland analysis of developmental EEG (MADE) pipeline. Psychophysiology. 2020 Jun;57(6):e13580.

57. Mognon A, Jovicich J, Bruzzone L, Buiatti M. ADJUST: An automatic EEG artifact detector based on the joint use of spatial and temporal features. Psychophysiology. 2011 Feb;48(2):229–240.

58. Nolan H, Whelan R, Reilly RB. FASTER: Fully Automated Statistical Thresholding for EEG artifact Rejection. J Neurosci Methods. 2010 Sep 30;192(1):152–162.

59. Goswami S, Cavalier S, Sridhar V, Huber KM, Gibson JR. Local cortical circuit correlates of altered EEG in the mouse model of Fragile X syndrome. Neurobiol Dis. 2019 Apr;124:563–572.

60. Chokron S, Kovarski K, Dutton GN. Cortical visual impairments and learning disabilities. Front Hum Neurosci. 2021 Oct 13;15:713316.

61. Macintyre-Béon C, Young D, Dutton GN, Mitchell K, Simpson J, Loffler G, et al. Cerebral visual dysfunction in prematurely born children attending mainstream school. Doc Ophthalmol. 2013 Oct;127(2):89–102.

62. Spierer A, Royzman Z, Kuint J. Visual acuity in premature infants. Ophthalmologica. 2004 Dec;218(6):397–401.

63. Edmond JC, Foroozan R. Cortical visual impairment in children. Curr Opin Ophthalmol. 2006 Dec;17(6):509–512.

64. Weinstein JM, Gilmore RO, Shaikh SM, Kunselman AR, Trescher WV, Tashima LM, et al. Defective motion processing in children with cerebral visual impairment due to periventricular white matter damage. Dev Med Child Neurol. 2012 Jul;54(7):e1–8.

65. Emberson LL, Boldin AM, Riccio JE, Guillet R, Aslin RN. Deficits in Top-Down Sensory Prediction in Infants At Risk due to Premature Birth. Curr Biol. 2017 Feb 6;27(3):431–436.

66. Fazzi E, Galli J, Micheletti S. Visual impairment: A common sequela of preterm birth. Neoreviews. 2012 Sep 1;13(9):e542–e550.

67. Ben Amor L, Chantal S, Bairam A. Relationship between late preterm birth and expression of attention-deficit hyperactivity disorder in school-aged children: clinical, neuropsychological, and neurobiochemical outcomes. RRN. 2012 Aug;77.

68. de Kieviet JF, van Elburg RM, Lafeber HN, Oosterlaan J. Attention problems of very preterm children compared with age-matched term controls at school-age. J Pediatr. 2012 Nov;161(5):824–829.

69. Fawcett SL, Wang Y-Z, Birch EE. The critical period for susceptibility of human stereopsis. Invest Ophthalmol Vis Sci. 2005 Feb;46(2):521–525.

70. Freeman RD, Ohzawa I. Development of binocular vision in the kitten's striate cortex. J Neurosci. 1992 Dec;12(12):4721–4736.

71. Jandó G, Mikó-Baráth E, Markó K, Hollódy K, Török B, Kovacs I. Early-onset binocularity in preterm infants reveals experience-dependent visual development in humans. Proc Natl Acad Sci USA. 2012 Jul 3;109(27):11049–11052.

72. Gyurkovics M, Clements GM, Low KA, Fabiani M, Gratton G. Stimulus-induced changes in 1/f-like background activity in EEG. J Neurosci. 2022 Aug 12;42(37):7144–7151.

73. Toda T, Homma D, Tokuoka H, Hayakawa I, Sugimoto Y, Ichinose H, et al. Birth regulates the initiation of sensory map formation through serotonin signaling. Dev Cell. 2013 Oct 14;27(1):32–46.

74. Altigani M, Murphy JF, Newcombe RG, Gray OP. Catch up growth in preterm infants. Acta Paediatr Scand Suppl. 1989;357:3–19.

75. Ribic A, Crair MC, Biederer T. Synapse-Selective Control of Cortical Maturation and Plasticity by Parvalbumin-Autonomous Action of SynCAM 1. Cell Rep. 2019 Jan 8;26(2):381–393.e6.

76. Wang B-S, Sarnaik R, Cang J. Critical period plasticity matches binocular orientation preference in the visual cortex. Neuron. 2010 Jan 28;65(2):246–256.

77. Toyoizumi T, Miyamoto H, Yazaki-Sugiyama Y, Atapour N, Hensch TK, Miller KD. A theory of the transition to critical period plasticity: inhibition selectively suppresses spontaneous activity. Neuron. 2013 Oct 2;80(1):51–63.

78. Chattopadhyaya B, Di Cristo G, Wu CZ, Knott G, Kuhlman S, Fu Y, et al. GAD67-mediated GABA synthesis and signaling regulate inhibitory synaptic innervation in the visual cortex. Neuron. 2007 Jun 21;54(6):889–903.

79. Gogolla N, Takesian AE, Feng G, Fagiolini M, Hensch TK. Sensory integration in mouse insular cortex reflects GABA circuit maturation. Neuron. 2014 Aug 20;83(4):894–905.

80. Carcea I, Patil SB, Robison AJ, Mesias R, Huntsman MM, Froemke RC, et al. Maturation of cortical circuits requires Semaphorin 7A. Proc Natl Acad Sci USA. 2014 Sep 23;111(38):13978–13983.

81. Pfeffer CK, Xue M, He M, Huang ZJ, Scanziani M. Inhibition of inhibition in visual cortex: the logic of connections between molecularly distinct interneurons. Nat Neurosci. 2013 Aug;16(8):1068–1076.

82. Panda S, Dohare P, Jain S, Parikh N, Singla P, Mehdizadeh R, et al. Estrogen Treatment Reverses Prematurity-Induced Disruption in Cortical Interneuron Population. J Neurosci. 2018 Aug 22;38(34):7378–7391.

83. Donato F, Rompani SB, Caroni P. Parvalbumin-expressing basket-cell network plasticity induced by experience regulates adult learning. Nature. 2013 Dec 12;504(7479):272–276.

84. Tierney A, Strait DL, O'Connell S, Kraus N. Developmental changes in resting gamma power from age three to adulthood. Clin Neurophysiol. 2013 May;124(5):1040–1042.

85. Reh RK, Dias BG, Nelson CA, Kaufer D, Werker JF, Kolb B, et al. Critical period regulation across multiple timescales. Proc Natl Acad Sci USA. 2020 Sep 22;117(38):23242–23251.

86. Arpino C, Compagnone E, Montanaro ML, Cacciatore D, De Luca A, Cerulli A, et al. Preterm birth and neurodevelopmental outcome: a review. Childs Nerv Syst. 2010 Sep;26(9):1139–1149.

87. Johnson S, Marlow N. Preterm birth and childhood psychiatric disorders. Pediatr Res. 2011 May;69(5 Pt 2):11R–8R.

88. Ribic A. Stability in the Face of Change: Lifelong Experience-Dependent Plasticity in the Sensory Cortex. Front Cell Neurosci. 2020 Apr 21;14:76.

89. Ye Q, Miao Q-L. Experience-dependent development of perineuronal nets and chondroitin sulfate proteoglycan receptors in mouse visual cortex. Matrix Biol. 2013 Aug 8;32(6):352–363.

90. Guan W, Cao J-W, Liu L-Y, Zhao Z-H, Fu Y, Yu Y-C. Eye opening differentially modulates inhibitory synaptic transmission in the developing visual cortex. Elife. 2017 Dec 11;6.

91. Komitova M, Xenos D, Salmaso N, Tran KM, Brand T, Schwartz ML, et al. Hypoxia-induced developmental delays of inhibitory interneurons are reversed by environmental enrichment in the postnatal mouse forebrain. J Neurosci. 2013 Aug 14;33(33):13375–13387.

92. van der Kooij MA, Ohl F, Arndt SS, Kavelaars A, van Bel F, Heijnen CJ. Mild neonatal hypoxia-ischemia induces long-term motor- and cognitive impairments in mice. Brain Behav Immun. 2010 Jul;24(5):850–856.

93. Salmaso N, Jablonska B, Scafidi J, Vaccarino FM, Gallo V. Neurobiology of premature brain injury. Nat Neurosci. 2014 Mar;17(3):341–346.

94. Castillo-Ruiz A, Hite TA, Yakout DW, Rosen TJ, Forger NG. Does birth trigger cell death in the developing brain? eNeuro. 2020 Feb 14;7(1).

95. Lacaille H, Vacher C-M, Penn AA. Preterm birth alters the maturation of the gabaergic system in the human prefrontal cortex. Front Mol Neurosci. 2021;14:827370.

96. Tibrewal M, Cheng B, Dohare P, Hu F, Mehdizadeh R, Wang P, et al. Disruption of Interneuron Neurogenesis in Premature Newborns and Reversal with Estrogen Treatment. J Neurosci. 2018 Jan 31;38(5):1100–1113.

97. Karnati S, Kollikonda S, Abu-Shaweesh J. Late preterm infants - Changing trends and continuing challenges. Int J Pediatr Adolesc Med. 2020 Mar;7(1):36–44.

98. Shapiro-Mendoza CK, Lackritz EM. Epidemiology of late and moderate preterm birth. Semin Fetal Neonatal Med. 2012 Jun;17(3):120–125.

99. Semple BD, Blomgren K, Gimlin K, Ferriero DM, Noble-Haeusslein LJ. Brain development in rodents and humans: Identifying benchmarks of maturation and vulnerability to injury across species. Prog Neurobiol. 2013 Aug;106-107:1–16.

606

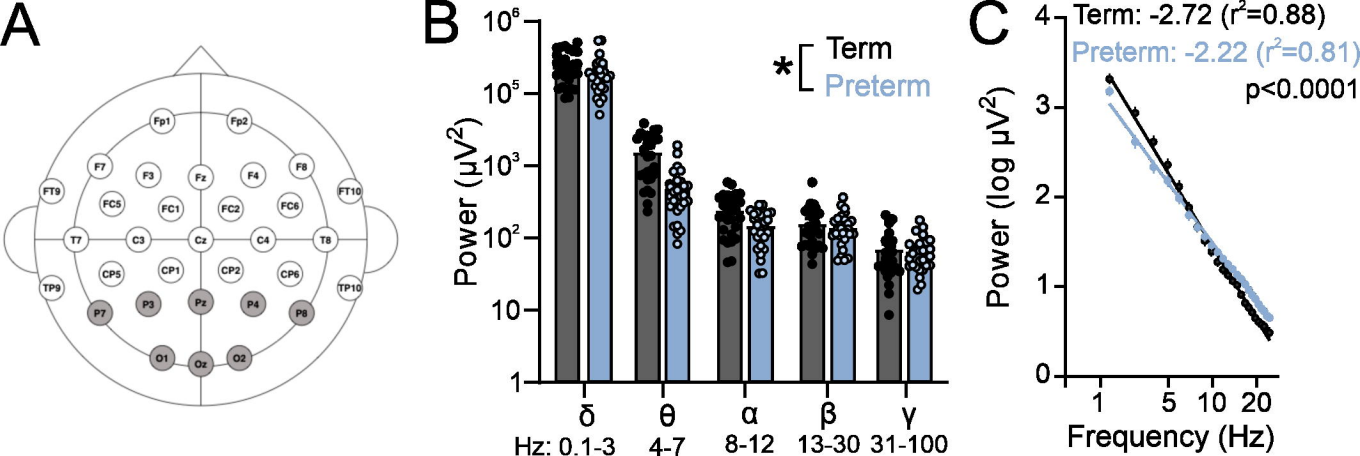
A
Fp1
Fp2
F7
F3
Fz
F4
F8
FT9
FT10
FC5
FC1
FC2
FC6
T7
C3
Cz
C4
T8
CP5
CP1
CP2
CP6
TP9
TP10
P7
P3
Pz
P4
P8
O1
Oz
O2
B
Power (μV²)
Term
Preterm
*
δ
θ
α
β
γ
Hz: 0.1-3
4-7
8-12
13-30
31-100
C
Term: -2.72 (r²=0.88)
Preterm: -2.22 (r²=0.81)
p<0.0001
Power (log μV²)
Frequency (Hz)

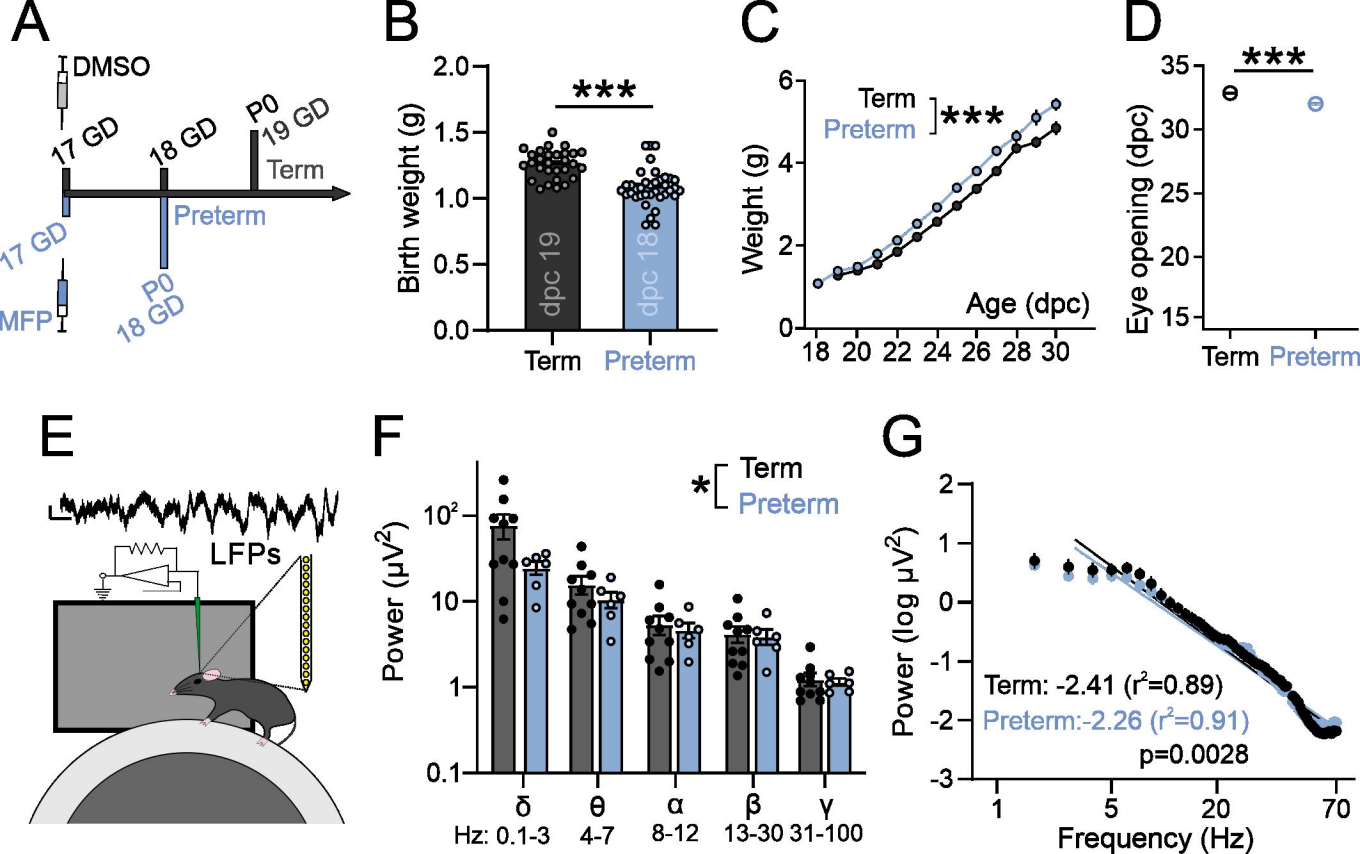
A
DMSO
17 GD
18 GD
P0
19 GD
Term
Preterm
17 GD
MFP
P0
18 GD
B
Birth weight (g)
2.0
1.5
1.0
0.5
0.0
***
dpc 19
dpc 18
Term
Preterm
C
Weight (g)
6
4
2
0
Term
Preterm
***
Age (dpc)
18 20 22 24 26 28 30
D
Eye opening (dpc)
35
30
25
20
15
***
Term
Preterm
E
LFPs
F
Power (μV²)
10²
10
1
0.1
*
Term
Preterm
δ
θ
α
β
γ
Hz: 0.1-3
4-7
8-12
13-30
31-100
G
Power (log μV²)
2
1
0
-1
-2
-3
Term: -2.41 (r²=0.89)
Preterm:-2.26 (r²=0.91)
p=0.0028
1
5
20
70
Frequency (Hz)

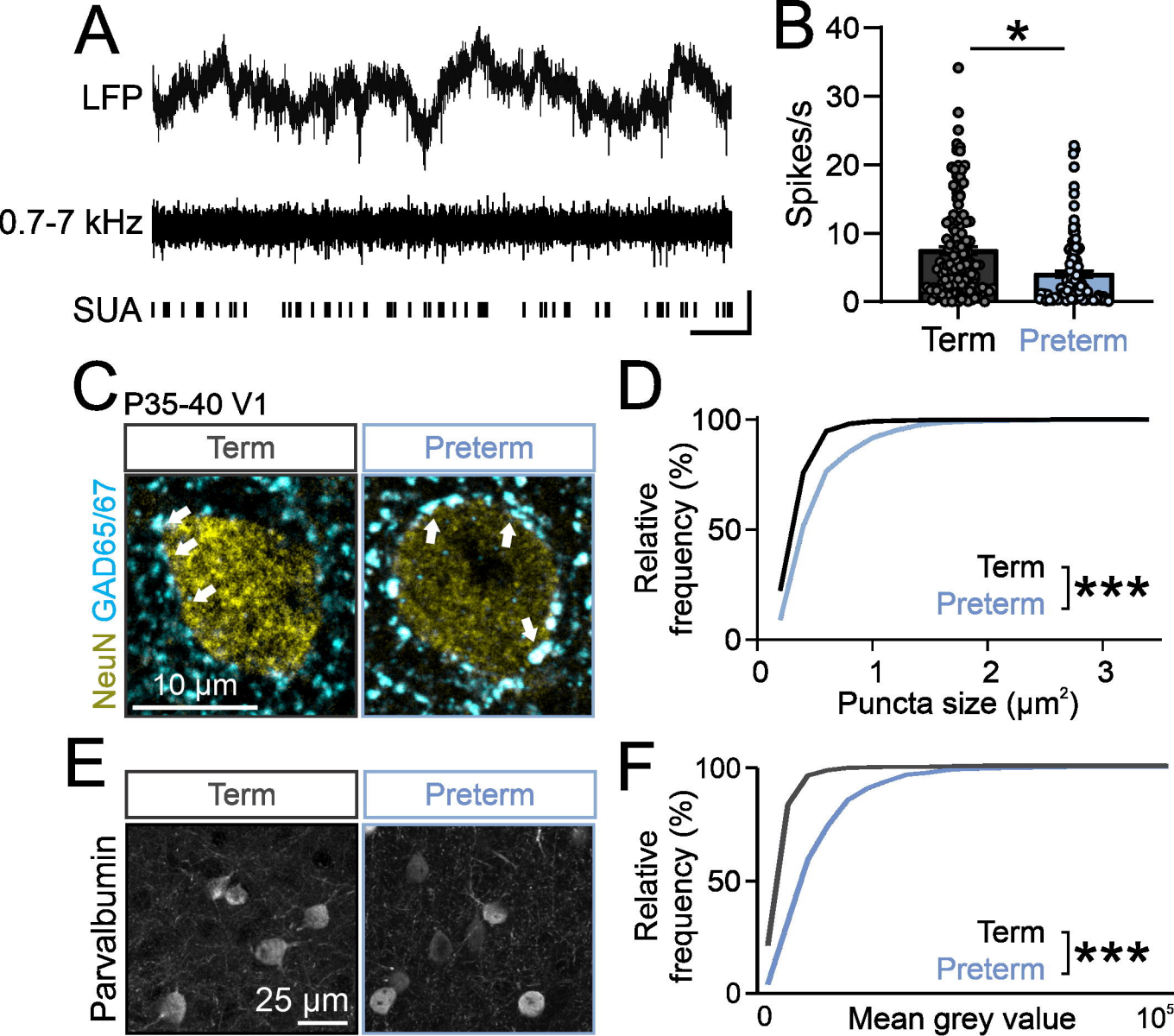
A
LFP
0.7-7 kHz
SUA
B
Spikes/s
40
30
20
10
0
*
Term
Preterm
C
P35-40 V1
Term
Preterm
NeuN GAD65/67
10 µm
D
Relative frequency (%)
100
50
0
Term
Preterm
***
0
1
2
3
Puncta size (µm²)
E
Term
Preterm
Parvalbumin
25 µm
F
Relative frequency (%)
100
50
0
Term
Preterm
***
0
Mean grey value
10⁵